Journal of Insect Physiology 54 (2008) 818–827

Contents lists available at ScienceDirect

Journal of Insect Physiology

journal homepage: www.elsevier.com/locate/jinsphys

Adhesive properties of the arolium of a lantern-fly, *Lycorma delicatula* (Auchenorrhyncha, Fulgoridae)

Leonid Frantsevich [a,b], Aihong Ji [a], Zhendong Dai [a], Jintong Wang [a], Ludmila Frantsevich [a,b], Stanislav N. Gorb [b,c,*]

[a] Institute of Bio-Inspired Structure and Surface Engineering, Nanjing University of Aeronautics and Astronautics, 29 Yudao Street, Nanjing 210016, China
[b] Schmalhausen-Institute of Zoology, B. Chmelnicky Street, 15, Kiev-30, 01601, Ukraine
[c] Evolutionary Biomaterials Group, Department of Thin Films and Biological Systems, Max-Planck-Institut für Metallforschung, Heisenbergstrasse 3, D-70569 Stuttgart, Germany

ARTICLE INFO

Article history:
Received 9 October 2007
Received in revised form
3 March 2008
Accepted 4 March 2008

Keywords:
Attachment devices
Adhesion
Friction
Insect locomotion
Stick-slip

ABSTRACT

The arolium in *Lycorma delicatula* is shaped as a truncated pyramid, tapering proximally. The base or the terminal area is corrugated, forming parasagittal wrinkles (period 1.5–5.0 μm), which are supported from inside by cuticular dendrites. Side faces of the arolium are made up of sclerotized dorsolateral plates. When claws slip on a smooth substrate and pronate, the dorsolateral plates diverge and expand the sticky terminal area. The real contact area with the glass plate was recognized by light reflection on its periphery. This area was measured and shown to be smaller when the leg was pressed perpendicularly to the substrate (0.02 mm^2) than when it was sheared in a direction parallel to the substrate (0.05 mm^2). Attachment forces were measured with the aid of dynamometric platforms during pulling of active insects from horizontal or vertical glass surfaces. Normal adhesive force (about 9–12 mN) was much less than friction force during sliding with velocity of 6–17 mm/s (50–100 mN); however, when expressed in tenacity per unit contact area the difference was less pronounced: 170 and 375–625 mN/mm^2, respectively. Sliding of the arolium during shear displacement was shown to be oscillatory in frame-by-frame video analysis. Relaxative oscillations consisted of periodical sticks-slips of the arolium along the glass surface.

1. Introduction

Adhesive pads of insect tarsi are adapted for holding onto smooth plant substrates, where claws fail to get a grip. The diversity of insect attachment pads was recently reviewed by Beutel and Gorb (2001, 2006). The arolium is an unpaired adhesive pad situated between the claws of the pretarsus. Arolii have been previously reported for representatives of Caelifera, Blattodea, Mantophasmatodea, Plecoptera, Auchenorrhyncha, Hymenoptera, Dermaptera, Mecoptera (Beutel and Gorb, 2001, 2006). In representatives of Auchenorrhyncha, these structures have been studied from the taxonomic or/and purely morphological viewpoint only (Haupt, 1935; Fennah, 1945; Doering, 1956; Emeljanov, 1987; Liang, 2002), and no experimental studies on arolium biomechanics in representatives of this insect group have been previously done. Some subtropical and tropical lantern-flies are rather large and presumably possess a strong adhesive ability. Additionally, their large body size makes them a convenient model object for force measurements and functional morphology studies of the pretarsus in general.

Lycorma delicatula White, 1845 inhabits eastern provinces of China. It lives openly on vegetation and possesses several adaptive features serving protective function against predators: (1) ability to jump, (2) cryptic coloration of forewings, (3) bright warning pattern of hind wings, and (4) warning posture with spread wings, which signals the toxicity of the insect (Xue and Yuan, 1996). *L. delicatula* bears sufficient ability to hold onto a vertical smooth glass or plastic wall and to move along the ceiling of a plastic cage. In the present paper, the structure of the arolium and its adhesive ability are studied. We present experimental data on maximal attachment forces and demonstrate different tenacity of the arolium in normal and tangential (shearing) directions relative to the substrate plane. The arolium structure and tenacity are compared to those previously studied in other insect taxa.

2. Methods

2.1. Insects

Adult *L. delicatula* were collected in September–October in the field. All experiments were carried out on freshly collected

* Corresponding author at: Evolutionary Biomaterials Group, Department of Thin Films and Biological Systems, Max-Planck-Institut für Metallforschung, Heisenbergstrasse 3, D-70569 Stuttgart, Germany. Tel.: +49 711 6893414; fax: +49 711 6893412.
E-mail addresses: leopup@izan.kiev.ua (L. Frantsevich), meeahji@nuaa.edu.cn (A. Ji), s.gorb@mf.mpg.de (S.N. Gorb).

0022-1910/$ - see front matter © 2008 Elsevier Ltd. All rights reserved.
doi:10.1016/j.jinsphys.2008.03.005

specimens. Because of the low survival rate in captivity (Lieu, 1934), freshly captured specimens were used only in one or two kinds of tests; new specimens were used in further tests. Individual insects were weighed after the experiments. We noticed that sticking abilities of adult *L. delicatula*, collected at the same site, obviously decreased until the end of the stated period; some individuals even possessed 1–2 black-colored rigid non-functional arolii.

2.2. Substrates

Leg placement was observed and video recorded on a glass plate, on outer surface of a glass cylinder (diameter 16 mm), and on the outer planar surface of a glass Petri dish (diameter 60 mm), both of which were glued to a plastic pedestal, total mass 25 and 22 g, respectively. The same substrates were used also for the force measurements.

2.3. Microscopy

Specimens were sacrificed by decapitation. Their legs were stored in distilled water in a refrigerator at 4 °C. After a few days, the legs with expanded arolii were taken out; their tarsi excised and fixed in 70° ethanol. Whole mounts of pretarsi were embedded in a glycerol–chloralhydrate–arabic gum medium and observed in an Olympus CX-41 light microscope equipped with an Olympus digital video camera C-4040. Images were stored with the aid of Olympus DP-Soft software (Olympus Corporation, Japan). In order to obtain high-quality images of the whole mounts, serial photographs of whole mounts at various focus depths were compiled using Helicon Focus software (Helicon Soft Ltd., Kharkov, Ukraine) in the Scientific Center of Ecology and Biodiversity (Kiev, Ukraine). For scanning electron microscopy, expanded arolii were dehydrated in an ascending series of ethanol solutions, dried by the critical point method, sputtercoated with gold–palladium to a thickness of 6 nm, and observed in an SEM Hitachi S-4800 with the use of a lower SE detector at the accelerating voltage of 3 kV.

2.4. Video recording

Insects were held by their wings and allowed to touch a smooth clean glass plate with their legs and grasp it. Leg placement was viewed from the ventral side with the aid of a Leica MZ 9.5 stereomicroscope; images and short video sequences were taken with the aid of a Moticam 1300 frame grabber and stored in a computer using Motic Images Advanced 3.1 software (Motic China Group Co., Ltd., China). Conventional video recordings were performed with a DCR-TRV325E camcorder (Sony Corporation, Japan) at the frame rate of 25 fps. Still frames were grabbed with the aid of AVIEdit software (AM Software, Moscow, Russia).

2.5. Dynamometry

For force measurements, we used dynamometric platforms of two types. The first one was the three-dimensional (3D) force platform, called here a 3D sensor, constructed by the Institute of Bioinspired Structure and Surface Engineering (resolution = 1 mN). The output of the sensor was fed online into a computer at the sampling frequency of 500 Hz (software Labview 6.1, National Instruments, USA). In our experiments, only the vertical force component was taken into account. The additional mass of the Petri dish slowed down the response of the sensor as a spring-mass system, and thus swift transients of its response were damped. The time constant was found by calibration to be 48 ± 5 ms (mean ± mean error).

The second dynamometric platform was the Mettler-Toledo AL204 electronic balance (Mettler-Toledo Group), connected to a computer with Balance-Link software. The substrate mass was set to zero. If the insect lifted the substrate, the output values were negative. Resolution of the balance was 1 μN in the static state. The sampling frequency (8 Hz) and time constant of the scales (240 ms) were found experimentally. Calibration revealed that the swift force transient was underscored by 15–25%. Room temperature during the force measurements was 27.0–28.5 °C at 70% relative humidity.

2.6. Data processing

Coordinates of some pretarsal structures, area, and perimeter of the arolium were measured from digital images with the aid of Sigma Scan Pro 5.0 software (SPSS Inc., Chicago, IL, USA). For the evaluation of the measurement error, two photographs were measured 10 times each. Standard deviation comprised 2–5% of the measured area. This error was considerably lower than variation in measurements between different samples (19% and 28%, respectively).

3. Results

3.1. Morphology

The length of the adult *L. delicatula* from the anterior margin of the head to the apex of the folded wing is 24.0–26.5 mm for females and 20.5–22.0 mm for males. Leg length was 18–22 mm in females and 15–18 mm in males. Average body mass, measured in 20 young adults, was 250 mg (range 180–325 mg). Females were considerably heavier than males.

The dorsal integument of the arolium is covered with small scales (10–20 μm long). When the arolium is not completely spread out, the dorsal surface forms several V-shaped wrinkles extended to the base of the arolium along the midline (Fig. 1(2)). The dorsal side of the arolium is flanked by a pair of heavily sclerotized dorsolateral plates (Figs. 2 and 3). The postero-medial corner of the plate converges closely to the claw, without an evident articulation. In front of the unguitractor plate, situated on the ventral side of the pretarsus, there is a zone of 10–12 rows of tapered scales. This zone is provisory referred below to as the planta. Ahead of the planta, there is a small, 40-μm long sclerite, easily noticeable in transparent whole mounts (Fig. 3). Its cuticle is slightly invaginated inside the arolium. Distally from the planta, the ventral integument of the arolium is covered with broad flat scales and longitudinal folds each of about 5-μm wide. It bears a pair of sensory hairs (socket 12 μm in diameter, base 5–6 μm, and length 20–22 μm). No other sensors were noticed in the arolium.

The distal face of the arolium represents an expandable flat oval sac, 600–700 μm × 170–185 μm, perimeter 1.5 mm, area 0.11–0.12 mm^2. We refer to this sack as the terminal lip adhering to the smooth substrate. The relief of the terminal lip is corrugated into regular vertical slits. Their period is about 5 μm in the transitory zone either in the dorsal or in the ventral regions of the arolium. Dividing dichotomously, slits form denser corrugations with the period of 1.5–3.0 μm in the middle of the ventral lip (Fig. 1(4,5)).

The arolium is filled up with an orange spongy mass occupying the upper, larger part of the arolium lumen, as it is seen in fractured SEM preparations (Fig. 1(6)). The dense cuticular

layer beneath the spongy mass serves as the basement for numerous cuticular dendrites, oriented at a skew to and connected with the outer integument of the terminal lip (Fig. 1(6)). Other pretarsal structures, such as the manubrium, arcus, auxillae, and pulvilli, were not found in the pretarsus of *L. delicatula* (Fig. 2).

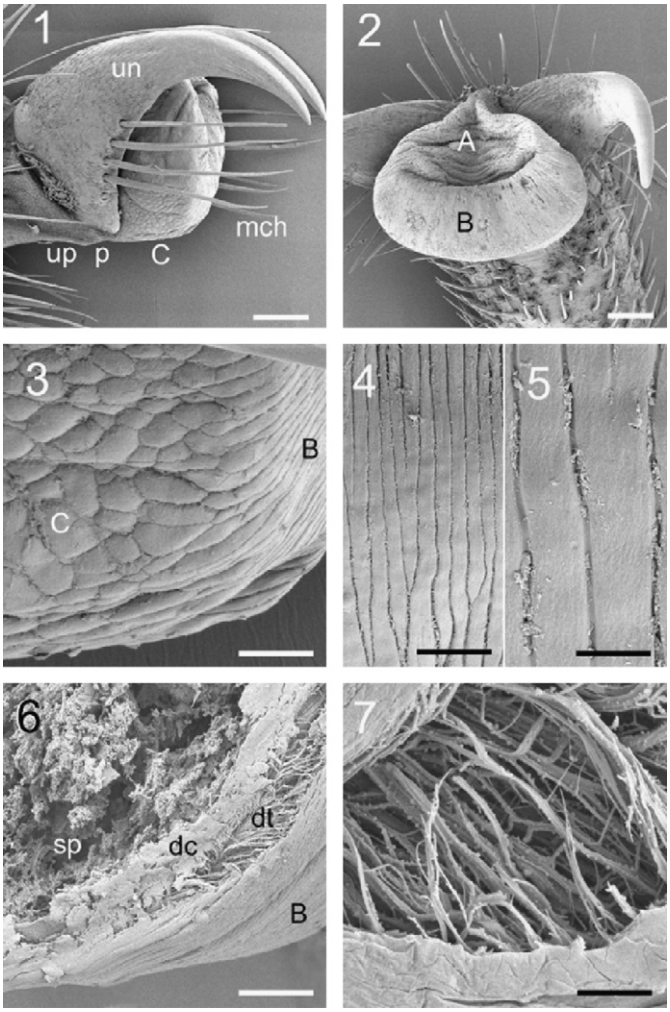

Fig. 1. Scanning electron micrographs of the pretarsus in *Lycorma delicatula*: 1, profile; 2, anterior view; 3, transition from the bottom side (C), covered with flat scales, to the terminal lip corrugated by vertical slits (B); 4, 5, vertical slits on the terminal lip; 6, fractured arolium, same zone as in 3; 7, dendritic layer. A, dorsal surface of the arolium; B, terminal sticky lip; C, bottom surface of the arolium. dc—dense cuticular layer; dt—dendritic layer; mch—setae; p—planta; sp—spongy mass; un—unguis (claw); up—unguitractor plate. Scale bars: 100 μm (1–2), 20 μm (4, 6), 10 μm (3), 5 μm (5), 2 μm (7).

3.2. Movements of the arolium

Retraction of claws in a fresh leg preparation was exerted by an inward pull, applied to the tendon of the claw retractor muscle, exposed in the tibia. During this action, the arolium bent down together with the claws. When the leg was placed on the substrate in a position similar to its natural position, the claws either interlocked with substrate irregularities in the case of a rough substrate, or slipped sideward on a smooth substrate during the tendon pull. In the first case, the arolium bent down only slightly, the terminal lip remained protected from the contact with the rough substrate. In the second case, inward excursion of the unguitractor was larger, as well as the bending of the arolium. The adhesive surface of the terminal lip contacted the smooth substrate. When claws slipped sideward and pronated, dorsolateral plates expanded the arolium. It was also possible to evert the terminal lip by applying pressure to the distal tarsomere with a fine forceps. This indicates a possible contribution of a hydraulic mechanism of the tarsus on the arolium unfolding.

3.3. Contact area

Insects were either placed on the glass plate from above (normal load) or dragged parallel to the plate, the legs being in contact with the plate (shear load). Insects used in both tests were not the same. Video sequences of the arolium, contacting glass by applying just normal load (Fig. 4) or normal load and shear (Fig. 5), demonstrated differences in the developed contact area. The contact area in legs, placed normally, was located predominantly at the proximal edge of the arolium or in its central part, while during shear, it was at the distal edge of the arolium and considerably larger than that at normal placement.

The real contact area was always smaller than the entire projected contact area of the arolium (Fig. 6; Tables 1 and 2). Real contact area was significantly larger when the load was applied in the shearing direction (t-test: $t_{average} = 17.2$; $t_{min} = 19.1$; $t_{max} = 8.28$; df = 68; $P_0 \ll 0.1\%$). Perimeters of the contact areas depicted in the Fig. 6 ranged from 1.0 to 1.5 mm. After multiple contacts with the glass plate, especially after shearing, the glass surface became covered with little drops of pad secretion.

3.4. Stick-slip behavior of the arolium during sliding

Video sequences of sliding arolia (Fig. 7) demonstrated that sliding motion, which seemed to be smooth at the frame frequency of 25 fps, appeared jerky in a careful frame-by-frame analysis. Average velocity of sliding was 0.26 mm/s. By lucky coincidence of both slip and frame frequencies, discrete slips of the arolium appeared in each third frame, whereas the leg stood still (stick phase) in the next two frames. Choosing a reference point, such as tiny light reflection on the claw tip, we were able to

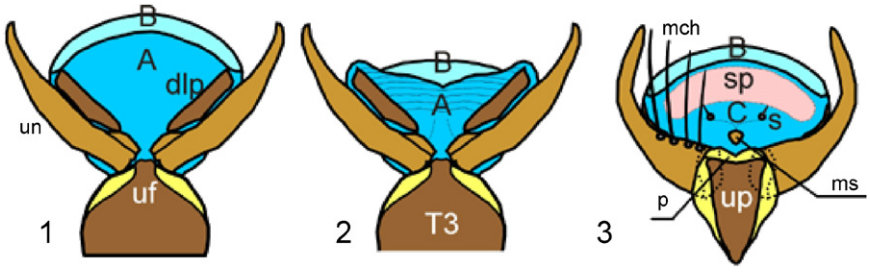

Fig. 2. Diagram of the arolium in *L. delicatula*: 1, dorsal side, arolium expanded; 2, dorsal side, arolium deflated; 3, ventral side, arolium expanded; A, dorsal surface of the arolium; B, terminal sticky lip; C, bottom surface of the arolium. dlp—dorsolateral plate, mch—setae; ms—ventral microsclerite; p—planta; s—mechanoreceptors (sensilla); sp—spongy material inside arolium; uf—unguifer; un—unguis (claw); up—unguitractor plate.

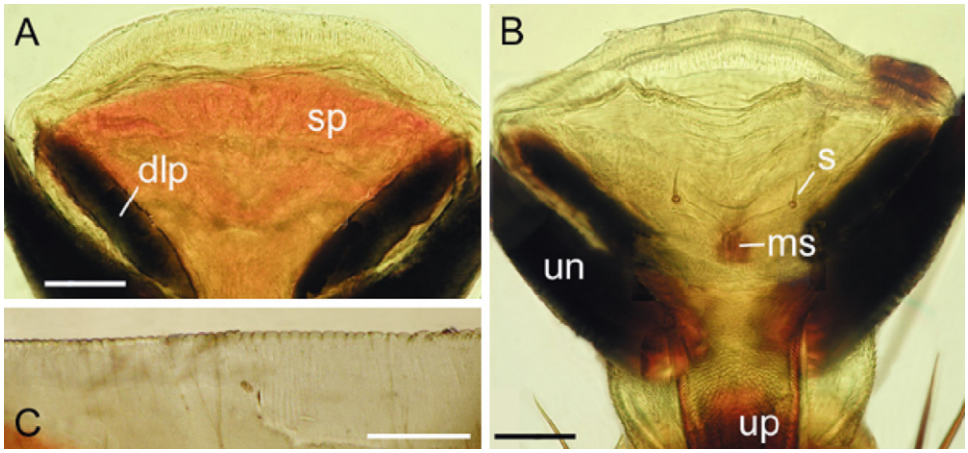

Fig. 3. Whole mounts of the arolium. (A) Dorsal side, orange spongy material is seen in the transparent specimen. (B) Ventral side, wrinkles of the partially deflated arolium are seen through the transparent cuticle. (C) Terminal lip with parallel slits at higher magnification. dlp—dorsolateral plate; ms—ventral microsclerite; s—mechanoreceptors (sensilla); sp—spongy material inside arolium; un—unguis (claw); up—unguitractor plate. Scale bars: 100 μm (A, B), 50 μm (C).

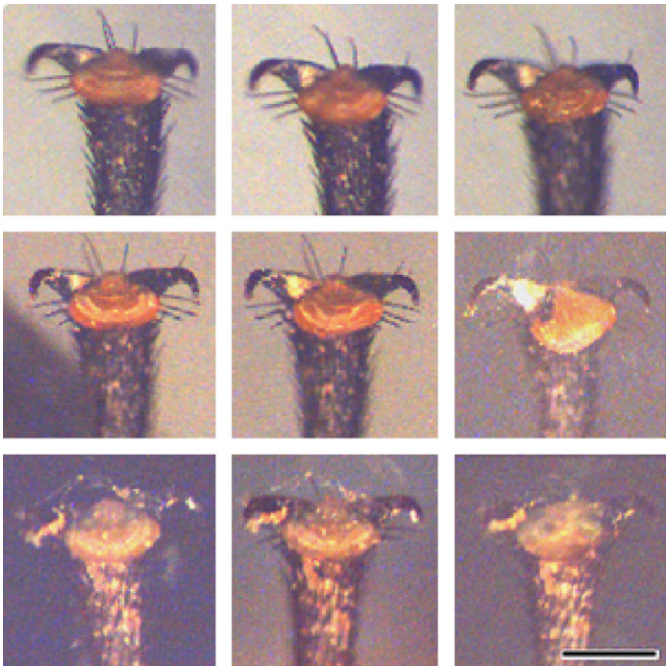

Fig. 4. Arolii of *L. delicatula* upon normal load on the glass plate. Still frames in rows from the left to the right are grabbed from different episodes on the same leg of the same animal. The real contact area is recognized by bright edge reflection. Claws are retracted and pronated, arolii and their contact areas at normal placement are pointing proximally. Scale bar: 0.5 mm.

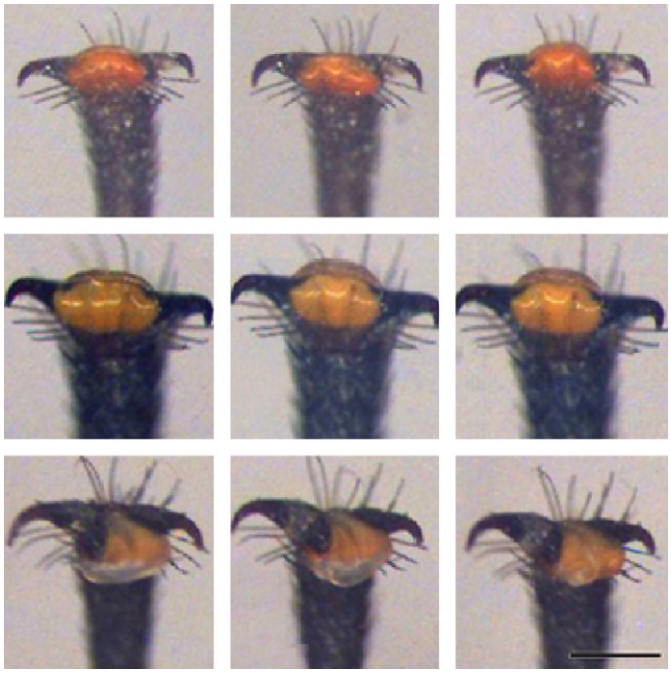

Fig. 5. Arolii of *L. delicatula* sliding along the glass plate. Still frames in rows from the left to the right are grabbed from different episodes on the same leg of the same animal. The real contact area is recognized by bright edge reflection. Claws are retracted and pronated, arolii and their contact areas during sliding point mostly distally. Scale bar: 0.5 mm.

trace the leg position frame-by-frame, totally in 376 frames. The analysis showed that the position of the reference point changed stepwise (Fig. 8). Periodicity of slips is seen better when we plot the difference in position between subsequent frames (δx). The negative values were obtained due to the pixelization error of about 1 pixel because the sparkle of the reference point was small (2–4 pixel) as well as the slips themselves (2–3 pixel, 20–30 μm). Periodicity was revealed statistically by the calculation of an autocorrelation function:

$$A = \frac{1}{T}\sum_{t=1^T} \sigma x(t)\sigma x(t+\tau),$$

where t is the time, τ the time lag between frames, T the total time of recording, all temporal units expressed as frame numbers. Autocorrelation values were normalized as linear correlation coefficients.

3.5. Force measurements

Ten insects were tested on the horizontal Petri dish and on the vertical cylinder (Fig. 9B). Ten other specimens were tested on the horizontal substrate with the use of the 3D sensor, and nine were tested on the vertical Petri dish (Fig. 9A). Ten replicates were made with each specimen on each substrate. Video recordings of seven episodes on the vertical substrate revealed that legs slide with an average velocity of 8.6 mm/s (range 6–17 mm/s). The angle between the substrate plane and applied force vector (from the wing base to the tarsi) was about 10°.

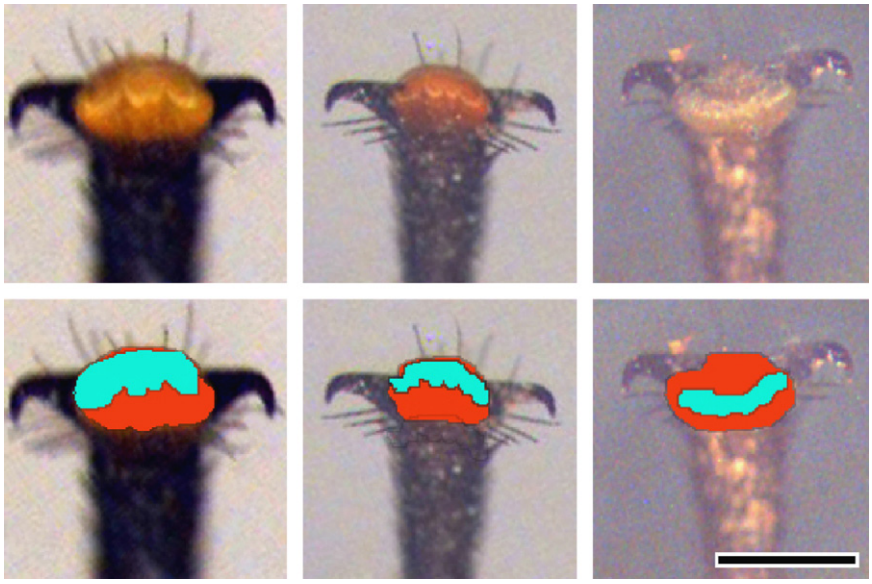

Fig. 6. The real contact area in arolii of *L. delicatula*. Upper row demonstrates single frames of sheared arolii. Lower row demonstrates same pictures, with the total projected area of the arolium colored in red and the real contact area colored in blue. Scale bar: 0.5 mm.

Table 1
Comparison of the whole average area and average contact area of the arolium on glass depending on the direction of applied force

Force direction	*N*	Whole area (mm^2)		Contact area (mm^2)		Contact area (%)	
		Mean	±SD	Mean	±SD	Mean	±SD
Normal	35	0.0701	0.0113	0.0215	0.0049	30.99	7.07
Shearing	55	0.1245	0.0236	0.0529	0.0150	42.41	9.02

Table 2
Limits of the whole and contact area of the arolium on glass

Force direction	*N*	Whole area (mm^2)		Contact area (mm^2)		Contact area (%)	
		Min	Max	Min	Max	Min	Max
Normal	35	0.0836	0.1536	0.0123	0.0471	14	43
Shearing	55	0.0701	0.1746	0.0202	0.0857	21	61

Force recordings were highly variable. They contained a positive force component when the insect legs were pressed to the substrate at the beginning of the experiment and a negative component when the adhered legs pulled the platform and lost their contact one by one (Fig. 10). Because of the variability in both duration and character of force curves in insects with intact legs, only extreme force values from each recording were taken into account. They usually corresponded to 2–4 legs being in contact with the glass surface.

Averaged extreme values of positive (load) and negative (adhesion or shear) forces are shown in Table 3. Shear forces were higher, almost by an order of magnitude, than adhesive forces in measurements on the horizontal planar and vertical cylindrical substrates ($t = 21.9$, df = 198, $P < 0.001$, t-test) and in measurements on the horizontal sensor and vertical planar glass ($t = 16.8$, df = 188, $P < 0.001$, t-test). We compared adhesion or friction forces averaged for each specimen with body mass of the same specimens and obtained negative values of correlation coefficients r, because adhesion and friction were considered as negative forces, and body mass was positive. The reason why linear regression lines were steeper in the first pair of experiments than in the second pair remains unclear.

Assuming the total contact area under shear load for three legs to be approximately 0.16 mm^2, and under normal load to be 0.06 mm^2, maximal shear force of 60–100 mN, and maximal adhesion force of 10 mN, we can derive a lateral (shear) tenacity of 375–625 kPa and a normal tenacity of 170 kPa. Power of frictional sliding, i.e., the work per second, at a velocity of 8 mm/s and force 50 mN comprised 0.4 mJ/s. This power dissipated along a path 8 by 1–2 mm (the last quantity is the total cross-section of leg contact areas).

4. Discussion

4.1. Morphology

Arolii are present in several suprafamilies of Cicadina, except singing cicadas. Emeljanov (1982) recognized three areas in the arolium of Cicadina: the top one, the bottom one, and the eversible terminal one. This situation is different from the orthopteroid arolium, lacking the eversible part (Slifer, 1950; Roth and Willis, 1952; Kendall, 1970), or that of mecopteroids, where the sticky area occupies the ventral side of the expanded arolium (Röder, 1986; Frantsevich and Gorb, 2002; Conde-Beutel et al., 2000; Federle and Endlein, 2004). The arolium in Cicadina is armored with several separate sclerites amidst the soft membrane. Spittle bugs Cercopoidea possess the most complex set of three pairs of plates equipped with sensory hairs. Adult Fulgoroidea possess only the dorsolateral pair of sclerites (Haupt, 1935; Emeljanov, 1987). The tiny ventromedial sclerite is reported here for the first time in lantern-flies. Its homology is unclear. The simplified arolium of lantern-flies resembles the thysanopteran arolium bearing dorsolateral sclerites (extenders) and eversible sticky terminal part (Emeljanov, 1987; Heming, 1972).

The eversible terminal lip in *L. delicatula* possesses parallel microscopical parasagittal wrinkles. Contacting surface of smooth adhesive pads of other insects is often non-smooth at the microscopical level: hexagonal (Orthoptera: Ensifera), striped by longitudinal or orthogonal lines (Hymenoptera, Mecoptera), complex wrinkles (Diptera: Tipulidae) (Gorb et al., 2002).

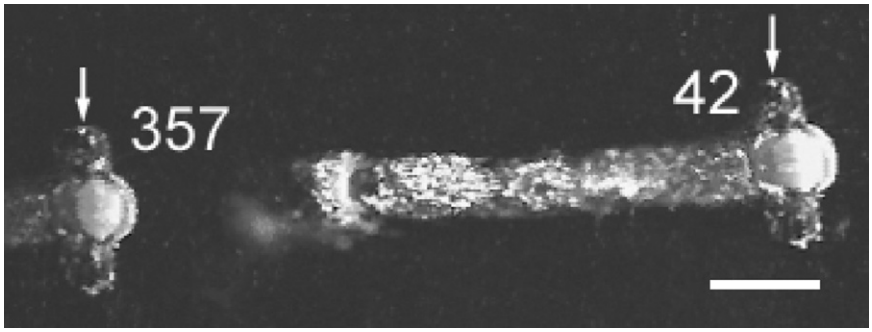

Fig. 7. Two superimposed frames of the video sequence of the arolium shear taken at the frequency of 25 fps. Frame numbers are indicated. Arrows point to the claw tip. Scale bar: 0.5 mm.

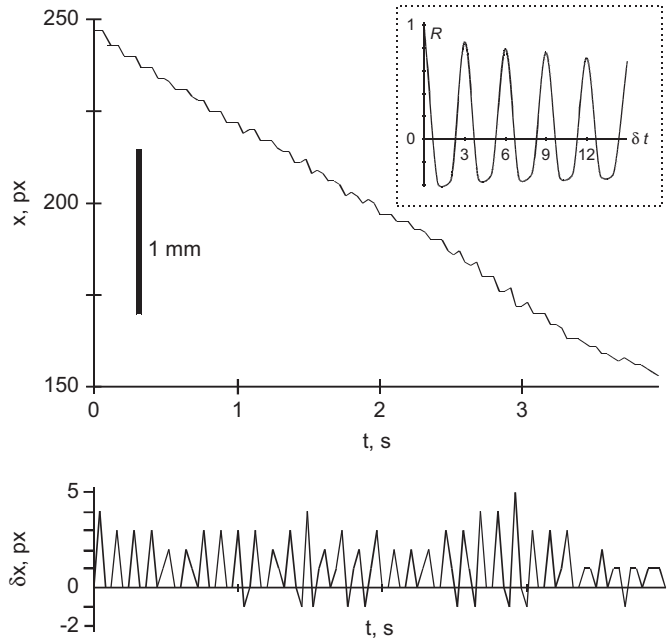

Fig. 8. Stick-slip behavior of the arolium on the glass plate. Upper graph shows an arolium displacement x in pixels versus time t (excerpt of 100 frames, scale bar: 1 mm). Bottom graph shows frame-to-frame shift δx in pixels versus time. Inset demonstrates an autocorrelation of frame-to-frame shifts expressed as linear correlation coefficient R versus time lag δt, which statistically reveals periodicity. Calculation of autocorrelation is based on 374 frames processed.

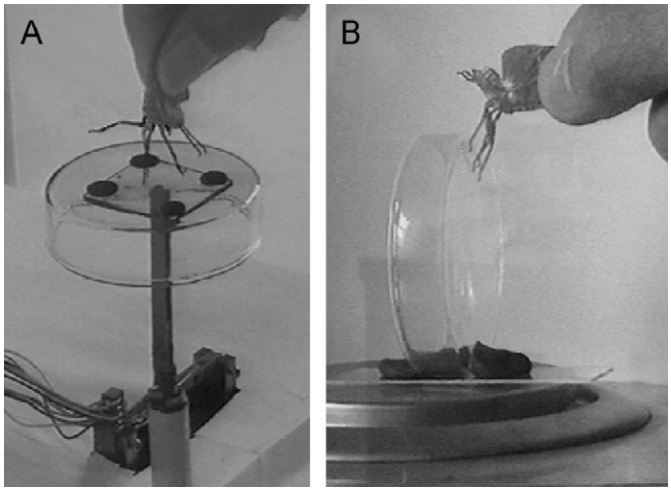

Fig. 9. Measurement of adhesion and friction of the arolii of *L. delicatula* on the glass surface. (A) Adhesion test: legs are brought in contact in the normal direction to the glass surface connected to the 3D sensor. (B) Friction test: legs are brought in contact in the shear direction; Petri dish is connected to the platform of an electronic balance.

Such contact splitting enhances van der Waals interaction even with the smooth substrate (Autumn et al., 2000; Scherge and Gorb, 2001; Arzt et al., 2003) and provides an additional pad adaptability to microscopic irregularities of the substrate. The outer splitting is supported by internal microstructure of underlining cuticle layers: rods with hierarchical branching pattern in arolii of cockroaches and grasshoppers (Roth and Willis, 1952; Slifer, 1950; Kendall, 1970), dendritic structures in euplantulae of bush crickets (Gorb and Scherge, 2000; Perez Goodwyn et al., 2006), and arolii of honeybees (Beutel and Gorb, 2001) and wasps (unpublished data of L.F. and S.G.). Arolium material in a spittle bug *Cercopis vulnerata* is foam-like, with the size of cells and thickness of their walls diminishing from the depth of the arolium to its surface. Elongated cells are oriented at some angle to the surface (Beutel and Gorb, 2001; Scherge and Gorb, 2001). Spongy cuticle has also been found in representatives of Thysanoptera (Heming, 1971). The lantern-flies studied here possess dendritic structures similar to those found in bush crickets, bees, and wasps.

Since the material of smooth pads is very soft (20–70 kPa; Gorb et al., 2000), it is rather sensitive to wear (Slifer, 1950). We have observed that adhesive properties of arolii of *L. delicatula* decrease with an increasing age of animals. This effect can be interpreted by wear. Additionally, ageing of adhesion structures may be caused by the stiffening of the material of soft pads as previously reported for arolii in cockroaches (Ridgel et al., 2003).

4.2. Kinematics

The principal mechanism of the actuation of the lantern-fly arolium on a smooth substrate is similar to those previously proposed by Snodgrass (1956) for the honeybee. If the claws do not grasp the substrate, they slip sideward and thus dilate the arolium. A turn of the claws, together with the arolium, was reported in fulgoroid cicadas from the family Dictiyopharidae (Emeljanov, 1982), in cockroaches (Roth and Willis, 1952; Frazier et al., 1999), and in the hornet *Vespa crabro* (Frantsevich and Gorb, 2002). During this action, the claws diverge and pronate. Such a claw movement results in a sideward pull of dorsolateral plate-like sclerites connected with the bottom side of the claws. Since the junction point is located far enough from the claw suspension point, the radius of divergence and pronation is of about 40% comparing to the claw length. Divergence of dorsolateral plates contributes to the arolium dilation, as it was previously supposed for thrips (Heming, 1972).

In addition to the lateral stretch, the terminal lip expands in contact with the substrate upon slight touch, as it has been earlier

demonstrated for arolii in the honeybee and the ant *Oecophila smaragdina* (Conde-Beutel et al., 2000; Federle and Endlein, 2004). Position and size of the real contact area in the sticky face of the arolium in the lantern-fly depend on the direction of the applied force while contacting the substrate.

Swelling of the *L. delicatula* arolium by an increased internal pressure was observed in cut-off tarsi placed in distilled water. However, it remains unclear whether the instant pressure change contributes to the reversible expansion of the arolium in physiological conditions. Arolium swelling was previously demonstrated in the honeybee (Conde-Beutel et al., 2000; Federle et al., 2001) and in the ant *Oecophila smaragdina* (Federle and Endlein, 2004) by applying pressure, and in the hornet (Frantsevich and Gorb, 2002) upon immersion in the hypotonic solution. It was previously supposed for adult thrips that stretching of the arolium by diverging claws together with an increased internal pressure, generated inside the tarsus, is responsible for the arolium evertion (Heming, 1971).

4.3. Secretion

In lantern-flies, pad secretion was observed as footprints on the glass surface. Pad secretion was previously observed in insects having different origin of sticky pads: smooth arolii in an ant *Oecophila smaragdina*, a stick insect *Carausius morosus*, a cockroach *Periplaneta americana* (Federle et al., 2002), a locust *Locusta migratoria* (Vötsch et al., 2002); plantulae in an aphid *Megoura viciae* (Lees and Hardie, 1988), and a bush cricket *Tettigonia viridissima* (Jiao et al., 2000); hairy pulvilli in the flies *Calliphora vomitoria* (Walker et al., 1985) and *Episyrphus balteatus* (Gorb, 1998), hairy tufts beneath the tarsomeres in a lady bird *Epilachna vigintioctomaculata* (Ishii, 1987), leaf beetle *Hemisphaerota cyanea* (Eisner and Aneshansley, 2000), and rove beetles *Stenus* spp. (Betz, 2003). Thickness of the secretion layer, which is essential for the generation of strong capillary adhesion, was evaluated to range from 18 to 2000 nm depending on the insect species and method used (Walker et al., 1985; Lees and Hardie, 1988; Eisner and Aneshansley, 2000; Schuppert and Gorb, 2006). Probably, leg sliding movements cause the thinning of the fluid film (Federle et al., 2002).

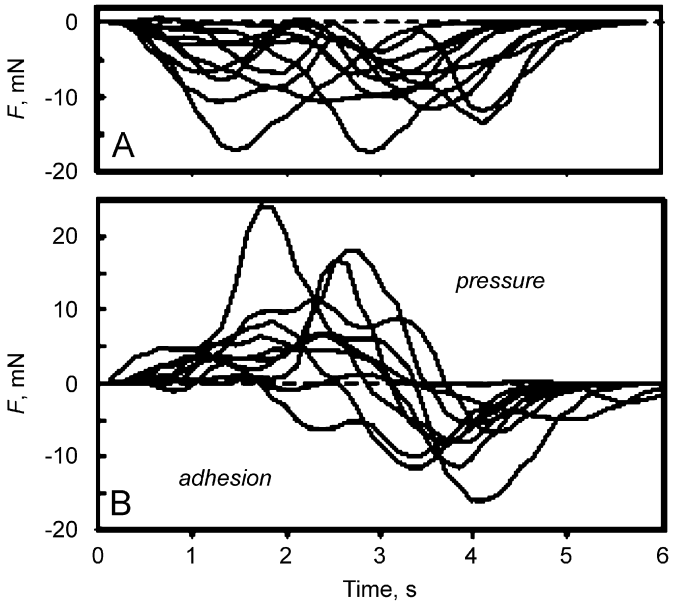

Fig. 10. Results of 20 single measurements of adhesive force of *L. delicatula* pulled off the flat platform of an electronic balance. (A) Shapes of responses, where only adhesive (negative peaks) component was revealed. (B) Complicated shapes of responses with initial pressure (positive peaks) and further adhesion. Fast components of the response are damped and smoothed due to high inertia of the platform.

4.4. Adhesion and friction

Adhesive forces of sticky pads were evaluated in different animals by the use of various methods: (1) by attaching loads to the animals walking on the smooth ceiling or wall (Ishii, 1987; Lees and Hardie, 1988; Frantsevich and Gorb, 2004; Eisner and Aneshansley, 2000), (2) by pulling the animal with a thread connected to the force sensor (Gorb, unpublished data), (3) by applying torsion or electronic balance (Walker et al., 1985; Lees and Hardie, 1988; Dixon et al., 1990; Eisner and Aneshansley, 2000; Frantsevich and Gorb, 2004), by evaluating the centrifugal force required to remove an insect from the horizontal or vertical surface of a centrifuge drum (Dixon et al., 1990; Federle et al., 2000; Gorb et al., 2001; Gorb and Gorb, 2004). Leaf beetle *Chrysolina polita* (Stork, 1980), rove beetles *Stenus* spp. (Betz, 2002), and various other insects (Gorb et al., 2004, 2005) actively pulled the thread attached to the force transducer.

Adhesion and shear force components are regarded as different physical phenomena: adhesion is the manifestation of an attractive force between two surfaces, whereas shear force is subdivided into static friction, the force preventing sliding along the substrate, and dynamic friction, the force acting against the motion if the specimen glides along the substrate (Scherge and Gorb, 2001). Biological adhesive mechanisms employ both types of forces (Walker et al., 1985; Autumn et al, 2000; Gorb et al., 2002). Adhesion in *L. delicatula* was of the same order of magnitude in two experiments with the 3D sensor and electronic balance: maximally about 9–12 mN (fourfold body weight), ordinarily 1.5–2 times less. Measurements for friction yielded values several times higher.

The ratio between friction and adhesion is rather high when both forces were compared in the same animal (Table 4) (see also Gorb et al., 2002). Both the size and the mass of animals shown in the table varied over a broad range: for example, areas of smooth pads varied from 0.004 to 0.02 mm^2 in tiny aphids to 0.8 mm^2 in the hornet *V. crabro*, and to 4.5 mm^2 in tree frogs. It was previously shown that ratio friction/adhesion linearly diminishes with increasing body mass in insects with hairy pads (Gorb et al., 2002): from 18 in the fruit fly *Drosophila melanogaster* (mass 3 mg), 10 in the leaf beetle *Gastrophysa viridula* (12–15 mg), 8 in the lady bird *Coccinella septempunctata* (25 mg), to 5 in the drone fly *Eristalis tenax* (60 mg).

Table 3
Maximal adhesion and friction forces and their correlation *r* with the body mass

Force direction and substrate	Instrument	Average force (mN)	Standard deviation	*N*	*r*
Adhesion, planar glass	Scales	−8.89	3.71	100	−0.79
Adhesion, planar glass	3D sensor	−12.03	6.58	100	−0.14
Shearing, glass cylinder	Scales	−54.25	20.44	100	−0.87
Shearing, planar glass	Scales	−96.39	47.25	90	−0.21

Table 4
Tenacity (friction or adhesion per unit of contact area) of smooth attachment pads on glass, in kPa (= mN/mm^2)

Taxon	Species	Organ	Tenacity	Direction	Reference
Blattodea	*Periplaneta americana*	Arolium	13–20	Normal	Roth and Willis (1952)
Orthoptera	*Tettigonia viridissima*	Euplantulae	1.7–2.2	Normal	Jiao et al. (2000)
	T. viridissima	Euplantulae	2–12	Normal	Perez Goodwyn et al. (2006)
	Locusta migratoria	Euplantulae	8–35	Normal	Perez Goodwyn et al. (2006)
Heteroptera	*Coreus marginatus*	Pulvilli	172	Shear	Gorb and Gorb (2004)
Aucheno rrhyncha	*Lycorma delicatula*	Arolium	170	Normal	This study
			375–625	Shear	
Sterno rrhyncha	*Aphis fabae*	Tibial euplantula	11	Normal	Dixon et al. (1990)
	Megoura viciae	Tibial euplantula	5–8	Normal	Lees and Hardie (1988)
			32	Shear	
Hymenoptera	*Vespa crabro*	Arolium	6	Normal	Frantsevich and Gorb, unpublished
	Oecophila smaragdina	Arolium	400	Shear	Federle et al. (2002)
Amphibia, Anura	*Osteopilus septentrionalis*	Pads on the toes	1.2	Normal	Hanna and Barnes (1991)
			30	Shear	

The values were either directly indicated in cited articles or derived from data of the cited authors, at least with precision of an order of magnitude. Friction was measured at velocities 8 mm/s for *L. delicatula* (this study), 2 mm/s for *O. smaragdina*, 2.5 mm/s for *O. septentrionalis* (Federle et al., 2002). Tenacity for cockroaches was calculated assuming their own weight as adhesion maximum, and the aroliar projection was taken as a total contact area (Roth and Willis, 1952).

Attachment and detachment of the contact zone between two solids wetted with fluid are complicated phenomena manifested at different scales. At the macroscale of force application, it is easier to hold onto a wall than to a ceiling. Depending on the number of legs in contact with the substrate and on the leg geometry, the applied force acts at a certain angle to adhesive organs. That is why there are two components (adhesive and frictional) acting on each single adhesive pad. The adhesive component is equal to P (applied external force). On the ceiling, normal force applied to the animal is the weight of the animal. On the wall, the normal force depends on the angle α between the substrate and the segment from the center of mass to the foothold (Daltorio et al., 2005), which requires the same two components (adhesion and friction), to keep adhesive contact in equilibrium. Adhesion component is directly proportional to $\tan\alpha$ and is small at a small value for α. Normal force in the wall situation is applied only at the upper (trailing) foothold.

Dynamic properties of adhesion and friction were investigated in several animals. A toe sticky pad of the tree frog *Osteopilus septentrionalis* glided on a smooth platform that moved laterally with controlled speed. Friction increased by six times upon an increase of velocity from 0.25 to 2.5 mm/s (Hanna and Barnes, 1991). In experiments on the grasshopper *T. viridissima*, friction was minimal at intermediate velocities and increased at lower and higher velocities (Gorb and Scherge, 2000). Time of hold on a ceiling depended upon time of constant weight action: in a leaf beetle *H. cyanea* it lasted over 2 min for 60 BWU (*body weight units*: ratio of the attachment force to own weight) but only a few seconds for 200 BWU (Eisner and Aneshansley, 2000). However, in most experiments on insects, velocity was not recorded (e.g., Walker et al., 1985; Stork, 1980).

Most investigators of adhesive pads of different animals such as tree frogs, flies, and geckos agree that detachment from the substrate is achieved predominantly by peeling (Hanna and Barnes, 1991; Niederegger and Gorb, 2003; Gao et al., 2005). The force required to cause peeling increases at acute peeling angles. The peeling model of a sticky rubber tape demonstrates the relationship between work of adhesion Wa and the sum of two terms: the potential energy term Wp and the elastic term We. The potential energy term Wp is related to the movement of an unexpandable tape upon an action of applied force F, which depends on the peeling angle α. The elastic term We is related to the expansion of the free piece of the tape, which does not depend on α (Kendall, 1975). Kendall equation, simplified for the unit area and unit width of a tape, is

$$W_a = F(1 - \cos\alpha) + \frac{F^2}{2dE},$$

where d is the thickness of the tape and E is Young's modulus. The last term becomes significant only for soft stretchable elastomeres. Kendall supposed that the force is constant at all peeling angles. He demonstrated that the peel strength at the right angle increased with an increasing crack velocity roughly as the cubic root of the velocity (in the range of 0.01–30 mm/s). In our study, we held the cicada by its wings and evaluated velocity from several video sequences.

Let us assume that the peeling speed and adhesion energy are constant, as well as the potential energy. In this case, the force is inversely proportional to $(1-\cos\alpha)$. Hence, at small peeling angles, the attachment force tends to infinity. This is a possible reason why friction forces in dragged insects are rather high (Gorb et al., 2002). This fact may explain long holding of two leaves during nest building in the weaver ant (Federle and Endlein, 2004), and difficulties in leg detachment if legs are too much extended in cockroaches (Roth and Willis, 1952) and hornets (unpublished data of L.F.).

Other reasons for high friction could be rather simple: (1) enhanced normal force resulting in the friction increase in the experiment with the glass cylinder and (2) difference in the contact area between substrate and legs tested in normal or shearing direction. The first assumption was rejected in the shear experiments on a flat substrate, while the second one appeared true, but only partially: the force per unit area (tenacity) was still larger for friction than for adhesion.

Attachment of biological adhesive pads may be explained by the contribution of intermolecular forces between the pad and substrate (dry adhesion) (Autumn et al., 2000), and due to surface tension and viscosity of the fluid in the contact zone (wet adhesion) (Hanna and Barnes, 1991; Langer et al., 2004). Presence of fluid suggests that dry adhesion is probably less important for the adhesive function of *Lycorma*'s arolium. Surface tension calculated for water (specific surface tension 0.71 mN/cm) at the maximal contact perimeter of the arolium comprises only 0.1 mN. It is not more than 0.4 mN for four legs attached to the glass surface. For fluids with surfactants, the calculated force might be even two times lower. It is far less than the weight of the lanternflies (2–3 mN).

In contrast to the surface tension, the viscous force depends on the total contact area. Force is inversely proportional to the time

of detachment and directly proportional to the fourth power of diameter (Bowden and Tabor (1950) cited by Lees and Hardie (1988)). Calculations of viscous force for aphids by Lees and Hardie (1988) and Dixon et al. (1990) differed by many orders of magnitude, because the authors presumed different time of separation (0.02 and 1 s), thickness of separating fluid (0.017 and 1 μm) and different viscosity of this fluid. Viscous effects act only during movement. They do not contribute to the static state in either direction: normal or shearing (Gorb et al., 2002; Federle et al., 2002, 2004). The cited authors emphasized that viscosity determines mostly lateral force, friction. In shear, the liquid under the arolium also acts as a lubricant at a certain thickness of the fluid layer and enables smooth gliding under action of an external force.

However, at the micro- and nanoscale, gliding is not steady. It may be an oscillatory stick-and-slip process of re-establishing and breakage of bonds between the pad and the substrate through an intermediate fluid layer or directly in the contact zone between two solids. Reshaping and fragmentation of the contact area are well possible. Stick-and-slip contact behavior was noticed long ago in everyday life: the creak of a tree in the woods, the sound of a violin, squeaking of the car brake, polymer sliding on the glass (Scherge and Gorb, 2001; Varenberg and Gorb, 2007).

Static hold appears to be of a dynamic nature upon scrutinized observation: fly's pulvilli slowly glide on the glass and need repositioning (Wigglesworth, 1987), loaded aphids on a wall slowly glide down (Lees and Hardie, 1988). Breakage of the contact also involves microscale events: local stress concentrations in the boundary area and formation of voids and cracks (Peressadko and Gorb, 2004; Ghatak et al., 2004). Molecular effects, such as reorientation of asymmetrical molecules of the fluid, may also contribute.

Acknowledgments

This study was supported by National Natural Science Foundation of China to ZD (Grant no. 60535020) and by Federal Ministry of Education, Science and Technology, Germany to S.G. (Project InspiRat 01RI0633D). Zhang Zhengjie and Liang Sheng assisted with video recordings and force measurements using the 3D sensor. We thank Prof. Dr. D. Denlinger and an anonymous reviewer for valuable improvements and suggestions.

References

Arzt, E., Gorb, S., Spolenak, R., 2003. From micro to nano contacts in biological attachment devices. Proceedings of the National Academy of Sciences of the USA 100, 10603–10606.

Autumn, K., Liang, Y.A., Hsieh, S.T., Zesch, W., Chan, W.P., Kenny, T.W., Fearing, R., Full, R.J., 2000. Adhesive force of a single gecko foot hair. Nature 405, 681–685.

Betz, O., 2002. Performance and adaptive value of tarsal morphology in rove beetles of the genus *Stenus* (Coleoptera, Staphylinidae). Journal of Experimental Biology 205, 1097–1113.

Betz, O., 2003. Structure of the tarsi in some *Stenus* species (Coleoptera, Staphylinidae): external morphology, ultrastructure, and tarsal secretion. Journal of Morphology 255, 24–43.

Beutel, R.G., Gorb, S.N., 2001. Ultrastructure of attachment specializations of hexapods (Arthropoda): evolutionary patterns inferred from a revised ordinal phylogeny. Journal of Zoological Systematics and Evolutionary Research 39, 177–207.

Beutel, R.G., Gorb, S.N., 2006. A revised interpretation of the evolution of attachment structures in Hexapoda with special emphasis on Mantophasmatodea. Arthropod Systematics and Phylogeny 64, 3–25.

Bowden, F.P., Tabor, D., 1950. The Friction and Lubrication of Solids. Oxford University Press, Oxford.

Conde-Beutel, R., Erickson, E.H., Carlson, S.D., 2000. Scanning electron microscopy of the honeybee, *Apis mellifera* L. (Hymenoptera: Apidae) pretarsus. International Journal of Insect Morphology and Embryology 24, 59–69.

Daltorio, K.A., Gorb, S., Peressadko, A., Horchler, A.D., Ritzmann, R.E., Quinn, R.D., 2005. A robot that climbs walls using micro-structured polymer feet. In: Proceedings of International Conference on Climbing and Walking Robots (CLAWAR), London, UK, pp. 131–138.

Dixon, A.F.G., Croghan, P.C., Gowing, R.P., 1990. The mechanism by which aphids adhere to smooth surfaces. Journal of Experimental Biology 152, 243–253.

Doering, K., 1956. The taxonomic value of the pretarsal structures in the classification of certain Fulgoroidea. The University of Kansas Science Bulletin 37, 627–644.

Eisner, T., Aneshansley, D.J., 2000. Defense by foot adhesion in a beetle (*Hemisphaerota cyanea*). Proceedings of the National Academy of Sciences of the USA 97, 6568–6573.

Emeljanov, A.F., 1982. Structure and evolution of tarsi in Dictyopharidae (Homoptera) (in Russ.). Entomologicheskoe Obozrenie 61, 501–516.

Emeljanov, A.F., 1987. Phylogeny of cicads (Homoptera, Cicadina) by comparative morphological data (in Russ). Trudy Vsesoyuznogo Entomologicheskogo Obschestva 69, 19–109.

Federle, W., Endlein, T., 2004. Locomotion and adhesion: dynamic control of adhesive surface contact in ants. Arthropod Structure and Development 33, 67–75.

Federle, W., Rohrseitz, K., Hölldobler, B., 2000. Attachment forces of ants measured with a centrifuge: better "wax-runners" have a poorer attachment to a smooth surface. Journal of Experimental Biology 203, 505–512.

Federle, W., Brainerd, E.L., McMahon, T.A., Hölldobler, B., 2001. Biomechanics of the movable pretarsal adhesive organ in ants and bees. Proceedings of the National Academy of Sciences of the USA 98, 6215–6220.

Federle, W., Riehle, M., Curtis, A.S.G., Full, R.J., 2002. An integrative study of insect adhesion: mechanics and wet adhesion of pretarsal pads in ants. Integrative and Comparative Biology 42, 1100–1106.

Fennah, R., 1945. Character of taxonomic importance in the pretarsus of Auchenorrhyncha (Homoptera). Proceedings of the Entomological Society of Washington 47, 120–128.

Frantsevich, L., Gorb, S., 2004. Structure and mechanics of the tarsal chain in the hornet, *Vespa crabro* (Hymenoptera: Vespidae): implications on the attachment mechanism. Arthropod Structure and Development 33, 77–89.

Frantsevich, L.I., Gorb, S.N., 2002. Arcus as a tensegrity structure in the arolium of wasps (Hymenoptera: Vespidae). Zoology 105, 225–237.

Frazier, S.F., Larsen, G.S., Neff, D., Quimby, L., Carney, M., Di Caprio, R.A., Zill, S.N., 1999. Elasticity and movements of the cockroach tarsi in walking. Journal of the Comparative Physiology A 185, 157–172.

Gao, H., Wang, X., Yao, H., Gorb, S., Arzt, E., 2005. Mechanics of hierarchical adhesion structures of geckos. Mechanics of Materials 37, 275–285.

Ghatak, A., Mahadevan, L., Chung, J.Y., Chandry, M.K., Shenoy, V., 2004. Peeling from a biomimetically patterned thin elastic film. Proceedings of the Royal Society of London A 460, 2725–2735.

Gorb, E., Kastner, V., Peressadko, A., Arzt, E., Gaume, L., Rowe, N., Gorb, S., 2004. Structure and properties of the glandular surface in the digestive zone of the pitcher in the carnivorous plant *Nepenthes ventrata* and its role in insect trapping and retention. Journal of Experimental Biology 207, 2947–2963.

Gorb, E.V., Haas, K., Henrich, A., Enders, S., Barbakadze, N., Gorb, S., 2005. Composite structure of the crystalline epicuticular wax layer of the slippery zone in the pitchers of the carnivorous plant *Nepenthes alata* and its effect on insect attachment. Journal of Experimental Biology 208, 4651–4662.

Gorb, S., Scherge, M., 2000. Biological microtribology: anisotropy in frictional forces of orthopteran attachment pads reflects the ultrastructure of a highly deformable material. Proceedings of the Royal Society of London B 186, 821–831.

Gorb, S., Jiao, Y., Scherge, M., 2000. Ultrastructural architecture and mechanical properties of attachment pads in *Tettigonia viridissima* (Orthoptera: Tettigoniidae). Journal of the Comparative Physiology A 186, 821–831.

Gorb, S., Gorb, E., Kastner, V., 2001. Scale effects on the attachment pads and friction forces in syrphid flies. Journal of Experimental Biology 204, 1421–1431.

Gorb, S.N., 1998. The design of the fly adhesive pad: distal tenent setae are adapted to the delivery of an adhesive secretion. Proceedings of the Royal Society of London B 265, 747–752.

Gorb, S.N., Gorb, E.V., 2004. Ontogenesis of the attachment ability in the bug *Coreus marginatus* (Heteroptera, Inecta). Journal of Experimental Biology 207, 2917–2924.

Gorb, S.N., Beutel, R.G., Gorb, E.V., Jiao, Y., Kastner, V., Niederegger, S., Popov, V.L., Scherge, M., Schwartz, U., Vötsch, W., 2002. Structural design and biomechanics of friction-based releasable attachment devices in insects. Integrative and Comparative Biology 42, 1127–1139.

Hanna, G., Barnes, W.J.P., 1991. Adhesion and detachment of the toe pads of tree frog. Journal of Experimental Biology 155, 103–125.

Haupt, K., 1935. Auchenorrhyncha. Die Tierwelt Mitteleuropas 4 (3), 115–443.

Heming, B.S., 1971. Functional morphology of the thysanopteran pretarsus. Canadian Journal of Zoology 49, 91–108.

Heming, B.S., 1972. Functional morphology of the pretarsus in larval Thysanoptera. Canadian Journal of Zoology 50, 751–766.

Ishii, S., 1987. Adhesion of a leaf feeding lady bird *Epilachna vigintioctomaculata* (Coleoptera: Coccinellidae) on a vertically smooth surface. Applied Entomology and Zoology 22, 222–228.

Jiao, Y., Gorb, S., Scherge, M., 2000. Adhesion measured on the attachment pads of *Tettigonia viridissima* (Orthoptera, Insecta). Journal of Experimental Biology 203, 1887–1895.

Kendall, K., 1975. Thin-film peeling-the elastic term. Journal of Physics D: Applied Physics 8, 1449–1452.

Kendall, M.D., 1970. The anatomy of the tarsi of *Schistocerca gregaria* Forskål. Zeitschrift für Zellforschung 109, 112–137.
Langer, M.G., Ruppersberg, J.P., Gorb, S.N., 2004. Adhesion forces measured at the level of a terminal plate of the fly's seta. Proceedings of the Royal Society of London B 271, 2209–2215.
Lees, A.D., Hardie, J., 1988. The organs of adhesion in the aphid *Megoura viciae*. Journal of Experimental Biology 136, 209–228.
Liang, A.-P., 2002. Seven new species of *Kinnara* Distant (Hemiptera: Fulgoroidea: Kinnaridae), with notes on antennal sensilla and wax glands. Zoological Studies (Beijing) 41, 388–402.
Lieu, K.O.V., 1934. External morphology and internal anatomy of a lantern-fly, *Lycorma delicatula*. In: 1933 Year Book Bur. Entomol. Hangchow, pp. 2–25.
Niederegger, S., Gorb, S., 2003. Tarsal movements in flies during leg attachment and detachment on a smooth substrate. Journal of Insect Physiology 49, 611–620.
Peressadko, A., Gorb, S.N., 2004. When less is more: experimental evidence for tenacity enhancement by division of contact area. Journal of Adhesion 80, 247–261.
Perez Goodwyn, P.P., Peressadko, A., Schwarz, H., Kastner, V., Gorb, S., 2006. Material structure, stiffness, and adhesion: why attachment pads of the grasshopper (*Tettigonia viridissima*) adhere more strongly than those of the locust (*Locusta migratoria*) (Insecta: Orthoptera). Journal of the Comparative Physiology A 192, 1233–1243.
Ridgel, A.L., Ritzmann, R.E., Schaefer, P.L., 2003. Effects of aging on behavior and leg kinematics during locomotion in two species of cockroach. Journal of Experimental Biology 206, 4453–4465.
Röder, G., 1986. Zur Morphologie des Praetarsus der Diptera und Mecoptera. Zoologische Jahrbücher, Abteilung für Anatomie und Ontogenie der Tiere 114, 465–502.
Roth, L.M., Willis, E.R., 1952. Tarsal structure and climbing ability of cockroaches. Journal of Experimental Biology 119, 483–517.
Scherge, M., Gorb, S.N., 2001. Biological Micro- and Nanotribology. Nature's Solutions. Berlin, Heidelberg, Springer.
Schuppert, J., Gorb, S., 2006. The wet step: visualisation of the liquid bridges in the attachment pads of the beetle *Gastrophysa viridula*. Society for Experimental Biology Main Meeting, University of Kent, Canterbury, 2–7 April 2006. Comparative Biochemistry and Physiology A 143 (Suppl. 1), Abstract no. A7.23.
Slifer, E.H., 1950. Vulnerable areas on the surface of the tarsus and pretarsus of the grasshopper (Acrididae, Orthoptera) with special reference to the arolium. Annals of the Entomological Society of America 43, 173–188.
Snodgrass, R.E., 1956. Anatomy of the Honey Bee. Comstock Publishing Associates, New York.
Stork, N.E., 1980. Experimental analysis of adhesion of *Chrysolina polita* (Chrysomelidae, Coleoptera) on a variety of surfaces. Journal of Experimental Biology 88, 91–107.
Varenberg, M., Gorb, S., 2007. Shearing of fibrillar adhesive microstructure: friction and shear-related changes in pull-off force. Journal of the Royal Society Interface 4, 721–725.
Vötsch, W., Nicholson, G., Müller, R., Stierhof, Y.-D., Gorb, S., Schwarz, U., 2002. Chemical composition of the attachment pad secretion of the locust *Locusta migratoria*. Insect Biochemistry and Molecular Biology 32, 1605–1613.
Walker, G., Yule, A.B., Ratcliff, J., 1985. The adhesive organ of the blowfly, *Calliphora vomitoria*: a functional approach (Diptera: Calliphoridae). Journal of Zoology London A 205, 297–307.
Wigglesworth, V.B., 1987. How does a fly cling to the under surface of a glass sheet? Journal of Experimental Biology 129, 373–376.
Xue, G., Yuan, S., 1996. Separation and preparation of indole alkaloids in *Lycorma delicatula* White by HPLC (in Chinese). Zhongguo Zhong Yao Za Zhi 21, 554–576.